

# Predictions of the Measurement Precision in Future Lensing Surveys

Erin S. Sheldon,<sup>1</sup>

## ABSTRACT

In this document I calculate the predicted sensitivity for DES. I extend the previous predictions to sensitivity as a function of source redshift for use in cosmic shear type studies, as well as sensitivity as a function of lens redshift for cross-correlation lensing studies. The framework presented is general, but I apply it directly to DES predictions.

## Contents

<b>1</b>	<b>Introduction</b>	<b>2</b>
<b>2</b>	<b>Signal and Noise</b>	<b>2</b>
2.1	Cosmic Shear . . . . .	3
2.2	Cross-correlation, or Object Lensing . . . . .	3
<b>3</b>	<b>Other Sources of Noise</b>	<b>4</b>
3.1	Cosmic Shear . . . . .	4
3.2	Cross-correlation Lensing . . . . .	4
<b>4</b>	<b>DES Predictions</b>	<b>5</b>
4.1	Predictions for Cosmic Shear . . . . .	5
4.2	Adding Other Filters . . . . .	8

---

<sup>1</sup>Department of Physics, New York University, 4 Washington Place, New York, NY 10003.

4.3	Effective Number Density as Function of Source Redshift . . . . .	8
4.4	Effective Number Density as Function of Lens Redshift . . . . .	8

<b>A</b>	<b>Appendix: Data</b>	<b>11</b>
----------	-----------------------	-----------

## 1. Introduction

The noise for a given lensing measurement depends basically on the number of sources, the variance in intrinsic shapes for that source population, and the noise on individual shape measurements. The signal depends on the the mass of the lensing matter and the redshift distributions of lenses and sources. Most calculations of the predicted signal-to-noise ratio (S/N) simply take these numbers at face value, which is adequate in many situations.

The most important factor left out of standard calculations is redshift dependent shear noise. Fainter source galaxies are noisier and are thus downweighted, as are smaller galaxies for which the PSF smearing is more significant. Both of these properties, faintness and smallness, are correlated with redshift.

This weighting effectively alters the source redshift distribution. Although this is a secondary consideration relative to determining the actual redshift distribution, it is important for interpreting, or predicting, very precise measurements. It is also important for cross-correlation lensing when the lens redshift is high enough that a large fraction of the sources get little weight.

In this paper I will show formulas that explicitly account for this weighting and apply them in predicting sensitivity in the Dark Energy Survey (DES). I'll discuss other sources of noise that aren't easily modeled or predicted and discuss how to account for these by normalizing to existing measurements.

## 2. Signal and Noise

I'll discuss two types of measurements, the simpler cosmic shear measurements and the more complex cross-correlation measurements. Cosmic shear is simpler because it is an angular correlation function which has no explicit noise weighting that depends on redshift.

## 2.1. Cosmic Shear

All cosmic shear measurements are essentially shear-shear correlation functions. The correlation between pairs at a given separation is calculated, which contains a convolution of the source galaxy redshift distribution with itself. In interpreting the signal, one estimates the redshift distribution of the sources and models the redshift distribution for the intervening matter and the correlation function of that intervening matter. To make predictions for a given survey one follows essentially the same approach, modeling the redshift distributions and underlying cosmology. This measurement involves integrals over the source redshift distribution such as (leaving out some terms for clarity):

$$S(r) = \eta A \int dz_L \int dz_S w(z_S) \chi(z_L, z_S) P(z_S), \quad (1)$$

where  $\eta$  is the number density of sources per unit area of sky,  $A$  is the area of the survey,  $\chi(z_L)$  is a geometrical factor, and  $w(z_S)$  is an inverse shear variance weight factor, which depends implicitly on source redshift because higher redshift galaxies are less precisely measured, as discussed in the introduction.

The usual approach is to account for this weighting simply by modifying the number density to be an effective density  $\eta_{eff}$ . This is equivalent to assuming the weight is not a function of source redshift, that all sources get the same weight, thus reducing the effective number density by some factor. The recovered signal when modeled, or the the predicted signal for a future survey, will be incorrect because the assumed  $w(z_S)$  is not included in the integral. The weight generally will reduce the signal because lower redshift sources get sheared less than higher redshift sources.

## 2.2. Cross-correlation, or Object Lensing

Consider a measurement of the mean mass of set of lenses, e.g. clusters in a richness range, or galaxies of a given luminosity. Let the lenses have redshift distribution  $N(z_L)$  and probability distribution of mass profiles  $P(M(R)|z_L)$ . Let the sources have angular density  $\eta$  and redshift probability distribution  $P(z_S)$ . Let the weight for a source-lens pair be  $w(z_L, z_S)$  as discussed in the introduction. Finally assume, for simplicity, that the mass is the observable (which it is not). Then the mean mass is given by

$$\langle M \rangle = \int dz_L N(z_L) \int dM P(M(R)|z_L) \int_0^{R_{200}(M)} dR \frac{2\pi R}{D^2(z_L)} \int dz_S \eta P(z_S) w(z_L, z_S) M(z_L, R). \quad (2)$$

The variance is essentially one over this formula with the weight squared and the mass replaced by  $(M - \langle M \rangle)^2$ .

Note, the actual observable is the shear  $\gamma$ , which is converted into the redshift-independent quantity  $\Delta\Sigma$ :

$$\Delta\Sigma \equiv \gamma \times \Sigma_{crit}(z_L, z_S) \quad (3)$$

and that quantity is averaged. The results for many sources are averaged for each lens, and the results for many lenses are averaged to get the mean  $\Delta\Sigma$ .

As with cosmic shear, part of the weight factor is an inverse variance weight that depends implicitly on source redshift. For cross-correlations there is an additional explicit dependence on lens and source redshift through  $\Sigma_{crit}$ :

$$w(z_L, z_S) = \frac{1}{(\sigma_{SN}^2 + \sigma_i^2)\Sigma_{crit}^2(z_L, z_S)} \quad (4)$$

Note when the lens redshift is high, so that a large fraction of the sources are downweighted or even in front of the lens, the resulting signal to noise is different than predicted ignoring these redshift dependencies.

### 3. Other Sources of Noise

#### 3.1. Cosmic Shear

#### 3.2. Cross-correlation Lensing

Additional noise in  $\Delta\Sigma$  comes from a number of sources. There are sources of noise that are not easily accounted for, such as added variance from corrections that must be applied to the  $\Delta\Sigma$  profiles. For example, some sources are clustered for the lenses and the correction factor must be calculated from the data. Also, to extract masses without modeling, the  $\Delta\Sigma$  radial profile must be inverted, which increases the noise.

I think it is better for our purposes to account for these sources of noise by normalizing the result to existing measurements rather than modeling them directly. In that case, all that matters for the prediction are the redshift distributions and weight factor  $w(z_L, z_S)$ . The redshift range for the lenses can be made relatively small such that the mass profiles will not vary significantly in the redshift bin. Then the mass within r200 is essentially an overall scaling.

Under these assumptions, the relevant quantity for scaling existing results to another

survey is then

$$S = \eta \int_{z_1}^{z_2} dz_L N(z_L) \int_0^{R_{200}(M)} dR \frac{2\pi R}{D(z_L)^2} \int dz_S P(z_S) w(z_L, z_S), \quad (5)$$

where I have just dropped factors that do not matter for the relative scaling. This can be compared, for example, to the existing results if the masses and profiles are close to the same.

#### 4. DES Predictions

The source and lens redshift distributions can be reasonably predicted for a survey such as DES based on deep redshift surveys. I will focus on predicting the shear noise, but will incorporate redshift distributions from other sources later. I currently have simulations based upon the GOODS data from which I can predict the weight as a function of magnitude given the noise and seeing properties of a given survey. When combined with photometric redshifts these weights can be used to predict lensing.

The effective number density in the proposal was the total integrated over source redshift:

$$\eta_{eff} = \eta \int dz_S P(z_S) w(z_S). \quad (6)$$

This is appropriate for predictions of cosmic shear sensitivity, but in order to model the result we also need  $w(z_S)$ . Also, for cross-correlation lensing we need to account for additional explicit weights as a function of lens and source redshift (see §2.2). Due to that weighting clusters at higher redshift will only use the fainter and smaller galaxies. The S/N for these measurements will be suppressed compared to the current predictions based just on the total  $\eta_{eff}$ .

##### 4.1. Predictions for Cosmic Shear

The mean relative weight as a function of i-band magnitude is shown in Figure 1 for a seeing of 0.9". The number density and effective number density as a function of i-band magnitude are shown in figure 2. Note, the unweighted number density is higher than it would be in an actual image because the catalogs were derived from HST images; most of the faint objects would simply not be detected, and they have a corresponding low weight.

The effective density, integrated over all magnitudes, is shown in figure 3 as a function of seeing.

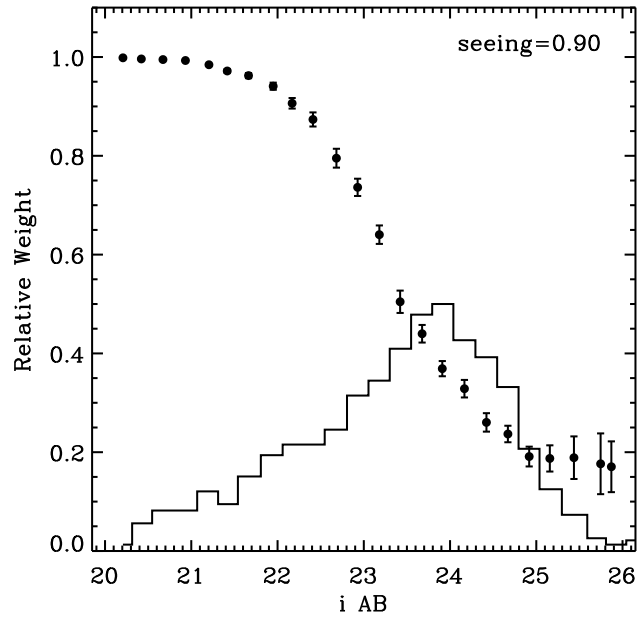


Fig. 1.— Relative weight as a function of i-band magnitude for seeing of 0.9". The histogram in magnitude is shown as the solid curve. Note, in practice objects will be cut at around  $i=24.1$ .

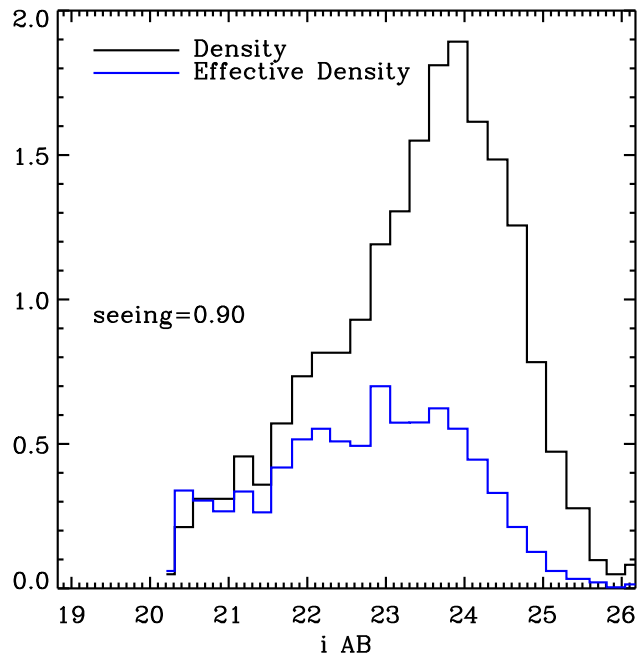


Fig. 2.— Number density and effective number density as a function of i-band magnitude for seeing=0.9"

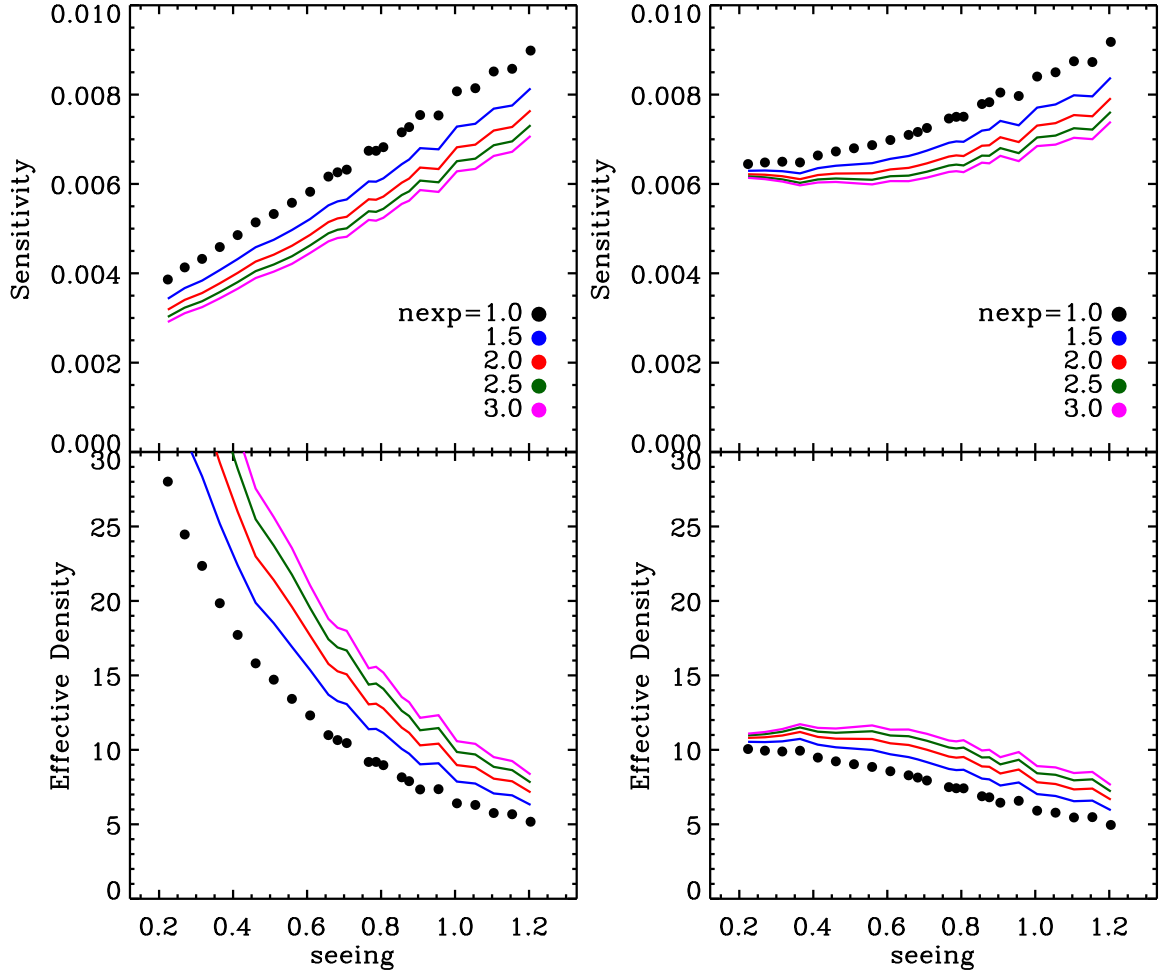


Fig. 3.— Left Panel: Effective density as a function of seeing with no explicit magnitude cut. Points are the des 5yr i-band predictions. Colored lines represent additional exposures from other bandpasses, where  $n_{\text{exp}}$  is the number of equivalent i-band sensitivity images. Right panel: Same as the left panel except with an explicit magnitude cut at  $i=24.1$ . In comparison with the left panel, this demonstrates the significant extra information at fainter magnitudes for very good seeing. The difference for typical seeing (0.9) is small.

## 4.2. Adding Other Filters

I estimated the expected improvement in the shape measurement error with more exposures, with an eye to including more bandpasses. Because the shape noise is unchanged when using the same objects with more images, the improvement in sensitivity is limited. Since there is no plan to coadd different bands, this is a good assumption. These curves are shown in the preceding figures and labeled by the number of effective 5 year i-band sensitivity images.

## 4.3. Effective Number Density as Function of Source Redshift

The effective number density as a function of source redshift can be calculated from  $\eta_{eff}(m_i)$  and an estimate of the redshift distribution in magnitude bins  $P(z_S|m_i)$ .

$$\eta_{eff}(z_S) = \int dm_i P(z_S|m_i) \quad (7)$$

Haun Lin has provided estimates of  $P(z_S|m_i)$  from **need details from Huan Here**. These estimates are shown in figure 4. I interpolated these curves to a finer grid of magnitudes in the calculationis that follow.

The resulting  $\eta_{eff}(z_S)$  for different seeing values, with an explicit magnitude cut at  $i=24.1$ , are shown in Figure 5.

## 4.4. Effective Number Density as Function of Lens Redshift

In order to calculate  $\eta_{eff}(z_L)$ , I re-calculated the sensitivity using the weights shown in Equation 4. For the source redshifts, I drew from the  $P(z_S|m_i)$  interpolated to a finer grid of magnitudes. This Monte Carlo was repeated 10 times and averaged. The results are shown in figure 6 for an explicit magnitude cut at  $i=24.1$ .



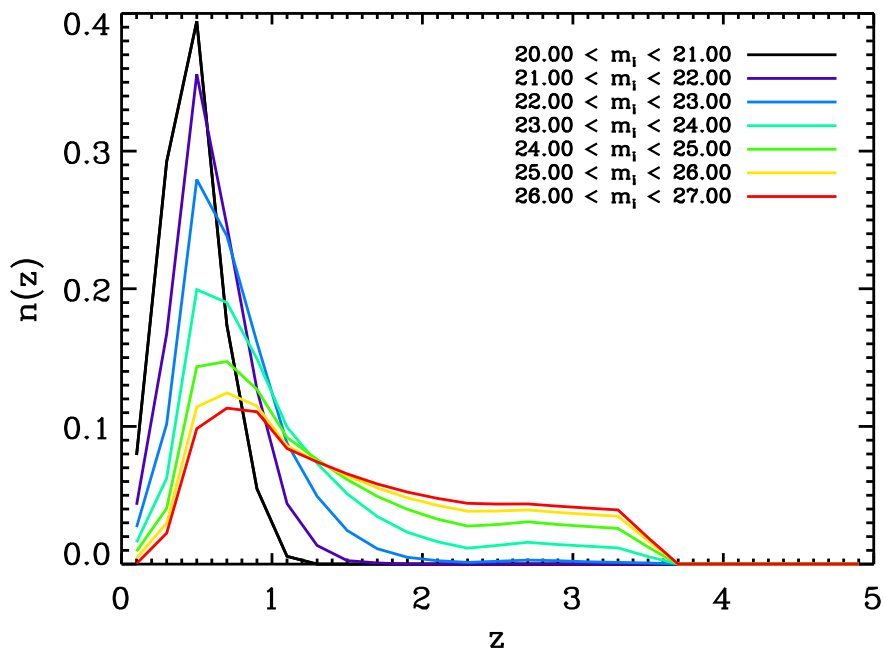


Fig. 4.— Estimated  $P(z_S|m_i)$  for DES from Huan Lin. **Need details.**

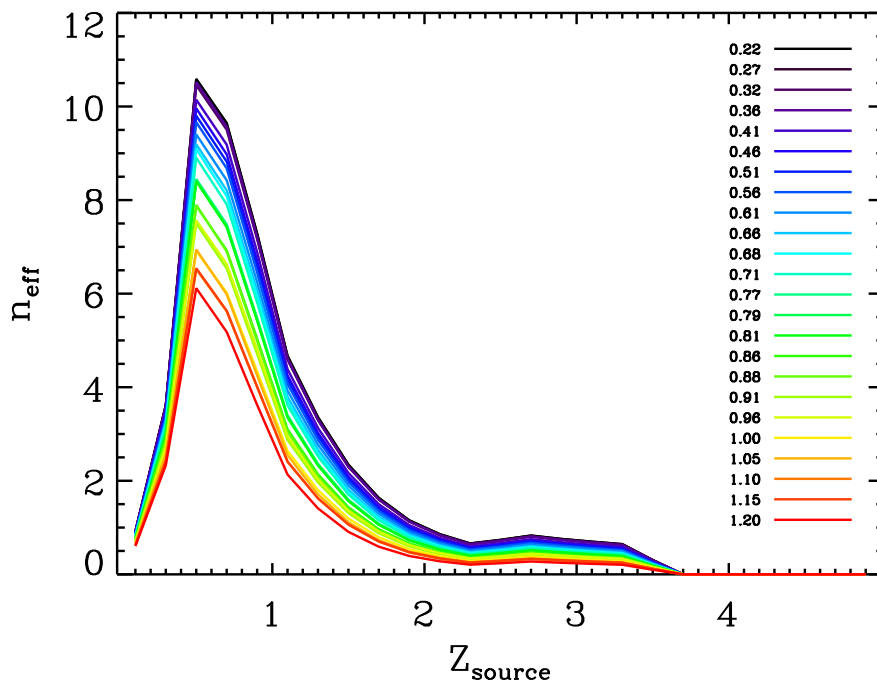


Fig. 5.— Effective density as a function of source redshift for a range of seeing values, calculated using the effective density as a function of magnitude from Figure 1 and the  $P(z_S|m_i)$  shown in figure 4. A cut was made at  $i=24.1$ .

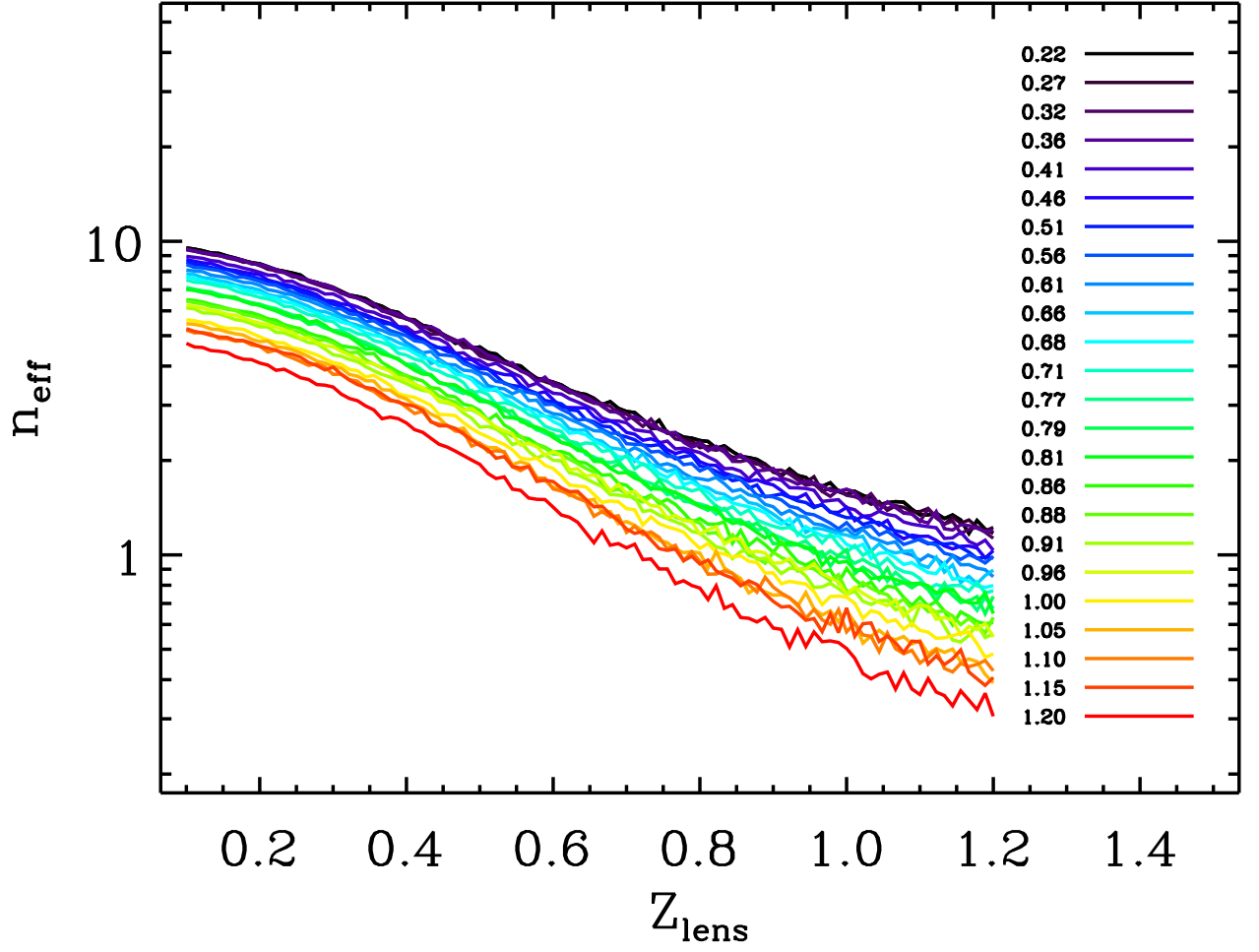


Fig. 6.— Effective density as a function of lens redshift for a range of seeing values. A cut was made at  $i=24.1$ . An explicit weighting with lens and source redshift is included as described in the text.

## A. Appendix: Data

Two FITS files containing predictions for DES 5yr i-band data are available from the Wiki. There is one with an explicit magnitude cut at  $i=24.1$  and one without. The files have the following structure as seen from an IDL perspective:

```
IDL> help,t30,/str
** Structure <b61498>, 26 tags, length=4832, data length=4828, refs=1:
SEEING          DOUBLE          0.22360680
MED_SEEING      DOUBLE          0.24474379
SHAPENOISE      DOUBLE          0.32000000
AREA            DOUBLE          61.295800
RAW_DENSITY     DOUBLE          77.574646
SHEAR_SENS      DOUBLE          0.0038612918
NEFF            DOUBLE          28.011993
SHEAR_SENS_SHONLY
                DOUBLE          0.0026181055
NEFF_SHONLY     DOUBLE          60.930533
SHEAR_SENS3     DOUBLE          0.0030886095
NEFF3           DOUBLE          43.780755
MULTI_NEXP      DOUBLE          Array[5]
MULTI_SENS_FAC  DOUBLE          Array[5]
MULTI_NEFF_FAC  DOUBLE          Array[5]
MAG_AUTO        DOUBLE          Array[35]
MWEIGHT         DOUBLE          Array[35]
MWEIGHT_ERR     DOUBLE          Array[35]
MHIST           LONG            Array[35]
MDENSITY        DOUBLE          Array[35]
MSHEAR_SENS     DOUBLE          Array[35]
MNEFF           DOUBLE          Array[35]
ZS              DOUBLE          Array[25]
ZSNEFF          DOUBLE          Array[25]
ZL              DOUBLE          Array[100]
ZLSENS          DOUBLE          Array[100]
ZLNEFF          DOUBLE          Array[100]
```

There is a row in the file for each value of seeing. Note that in IDL, long is a 32-bit integer.

The actual median seeing in the images is `MED_SEEING`. The total effective source density per square arcminute is `NEFF`. The sensitivity in the GOODS images, from which `NEFF` was derived, is `SHEAR_SENS`. The magnitude-dependent density is `MNEFF`, and the corresponding magnitude bins are `MAG_AUTO`. The weights as a function of magnitude are `MWEIGHT`.

For the effective density as a function of source redshift see the `ZS` and `ZSNEFF` tags. Similarly, for effective density as a function of lens redshift see `ZL` and `ZLNEFF`.

For adding calculating the effect of more exposures, see the `MULTI_*` tags in the data files as described in the appendix. The number of exposures is `MULTI_NEXP` and the corresponding factor for converting the single exposure density to multiple exposure density is `MULTI_NEFF_FAC`, and similar for sensitivity. This is somewhat different for different seeing values, so be sure to use the appropriate values.